TP-River

Monitoring and Quantifying Total River Runoff from the Third Pole

Lei Wang, Tandong Yao, Chenhao Chai, Lan Cuo, Fengge Su, Fan Zhang, Zhijun Yao, Yinsheng Zhang, Xiuping Li, Jia Qi, Zhidan Hu, Jingshi Liu, and Yuanwei Wang

ABSTRACT: Monitoring changes in river runoff at the Third Pole (TP) is important because rivers in this region support millions of inhabitants in Asia and are very sensitive to climate change. Under the influence of climate change and intensified cryospheric melt, river runoff has changed markedly at the TP, with significant effects on the spatial and temporal water resource distribution that threaten water supply and food security for people living downstream. Despite some in situ observations and discharge estimates from state-of-the-art remote sensing technology, the total river runoff (TRR) for the TP has never been reliably quantified, and its response to climate change remains unclear. As part of the Chinese Academy of Sciences' "Pan-Third Pole Environment Study for a Green Silk Road," the TP-River project aims to construct a comprehensive runoff observation network at mountain outlets (where rivers leave the mountains and enter the plains) for 13 major rivers in the TP region, thereby enabling TRR to be accurately quantified. The project also integrates discharge estimates from remote sensing and cryosphere–hydrology modeling to investigate long-term changes in TRR and the relationship between the TRR variations and westerly/monsoon. Based on recent efforts, the project provides the first estimate (656 ± 23 billion m^3) of annual TRR for the 13 TP rivers in 2018. The annual river runoff at the mountain outlets varies widely between the different TP rivers, ranging from 2 to 176 billion m^3, with higher values mainly corresponding to rivers in the Indian monsoon domain, rather than in the westerly domain.

KEYWORDS: Rivers; Streamflow; Climate change; Remote sensing; Surface observations; Hydrologic models

AFFILIATIONS: L. Wang, T. Yao, and F. Zhang—Key Laboratory of Tibetan Environment Changes and Land Surface Processes, Institute of Tibetan Plateau Research, Chinese Academy of Sciences, and University of Chinese Academy of Sciences, and CAS Center for Excellence in Tibetan Plateau Earth Sciences, Beijing, China; Chai, Qi, and Y. Wang—Key Laboratory of Tibetan Environment Changes and Land Surface Processes, Institute of Tibetan Plateau Research, Chinese Academy of Sciences, and University of Chinese Academy of Sciences, Beijing, China; Cuo, Su, Y. Zhang, and Li—Key Laboratory of Tibetan Environment Changes and Land Surface Processes, Institute of Tibetan Plateau Research, Chinese Academy of Sciences, and CAS Center for Excellence in Tibetan Plateau Earth Sciences, Beijing, China; Yao—Institute of Geographic Sciences and Natural Resources Research, Chinese Academy of Sciences, Beijing, China; Hu—Information Center, Ministry of Water Resources, Beijing, China; Liu—Key Laboratory of Tibetan Environment Changes and Land Surface Processes, Institute of Tibetan Plateau Research, Chinese Academy of Sciences, Beijing, China

River runoff at locations where rivers leave the mountains and enter the plains (mountain outlets) is an important hydrological parameter, representing the integrated output of the hydrological cycle at the mountainous headwaters of river basins. Monitoring changes in river runoff at mountain outlets is particularly important at the Third Pole (TP) because rivers in this region support millions of people in Asia (CIESIN 2018) and are very sensitive to climate change.

The TP, also known as the "Asian Water Tower," is a mountainous region of Asia centered on the Tibetan Plateau, where around $100{,}000\ \mathrm{km}^2$ of glaciers provide a critical freshwater supply to surrounding countries (Qiu 2008; Immerzeel et al. 2010; Yao et al. 2012a). Over the most recent half century, the TP has warmed at a significantly higher rate than other regions at the same latitude. The rate of warming at the TP is approximately twice the global average over this period (Chen et al. 2015), and there has been an increase in convective precipitation over the central TP region and a decrease in precipitation over the monsoon-impacted southern and eastern TP region (Yang et al. 2014). Rising temperatures at the TP have intensified melting, driving glacial retreat and frozen soil degradation, and have accelerated the regional water cycle (Li et al. 2008; Kang et al. 2010; Bibi et al. 2018; Ji and Yuan 2018; Wang et al. 2018; Yuan et al. 2018; Yao et al. 2019; Sun et al. 2020), which increases uncertainties associated with expected river runoff, and may change the spatial–temporal distribution of water resources (Cuo et al. 2014; Luo et al. 2018; Tang et al. 2019; Zhao et al. 2019). The impact of human activities on the TP environment has increased over recent decades, increasing uncertainties for the simulation and prediction of regional water resources, and affecting how they can best be utilized and managed. Changes and uncertainties in the total river runoff (TRR) from the TP, driven by both natural and anthropogenic forces, may threaten water supply and food security for millions of people living locally (57.2 million in 2015, and 59.3 million in 2020 for the mountain-outlet watersheds of the 13 studied rivers; population calculated from the Gridded Population of the World version 4 data collection; CIESIN 2018) and downstream, and may restrict the sustainable regional development of the ecological environment and the economy (e.g., Yao et al. 2013a; Biemans et al. 2019).

Routine ground-based hydrometeorological observations are sparse at the TP, which makes hydrology studies challenging, and it is difficult to make reliable estimates of TRR changes. First, it is hard to collect existing observations of discharge from many countries around the TP due to strict international and national data policies for river data. Second, the high elevation and harsh environment make it difficult and expensive to build and maintain new hydrological observation sites at the TP. Third, there is a lack of long-term high-mountain hydrological observations (e.g., river discharge, glacier, snow, and frozen ground) for most river basins at the TP, and this has constrained the development and validation of cryo-sphere–hydrology models. Fourthly, remote sensing images are constrained by instruments'

temporal and/or spatial resolution, and cannot provide continuous and reliable estimates of discharge for rivers in the high mountains of the TP region. It is therefore crucial that we strengthen the ground-based observation network for rivers at the TP to establish an integrated discharge-monitoring network that will allow us to acquire data that will provide fundamental support for scientific research and for sustainable socio-economic development. Existing hydrometeorological experiments and measurements made at the TP (e.g., Koike et al. 1999; Ma et al. 2008; Xu et al. 2008; Su et al. 2011; Li et al. 2013; Yang et al. 2013; Zhao et al. 2018) should be used as additional data sources for cryosphere–hydrology model inputs and model validation, and to improve our understanding of TP river basins.

Until now, despite some in situ observations of discharge and state-of-the-art technology (e.g., discharge estimates from remote sensing), the TRR for the high-elevation TP has not been reliably quantified and the TRR response to climate change remains unclear. Here, the TP-River project addresses these uncertainties as part of the "Pan-Third Pole Environment Study for a Green Silk Road (Pan-TPE)" program of the Chinese Academy of Sciences (CAS). The TP-River project aims to construct a comprehensive runoff observation network at the mountain outlets of the eight transboundary rivers of the TP (Mekong, Salween, Brahmaputra, Ganges, Indus, Amu Darya, Syr Darya, and Ili). Combining these observations with discharge estimates from remote sensing and cryosphere–hydrology modeling will enable the TRR to be accurately quantified for 13 major TP rivers, and will facilitate assessment of the TRR response to variations in the monsoon and in westerly winds.

Project design
Major rivers in the Third Pole region. This study will focus on quantifying changes in runoff at the mountain outlet locations for 13 major rivers in the Third Pole (TP) region, as shown in Fig. 1. These rivers include five Chinese rivers (the Yellow, Yangtze, Tarim, Shule,
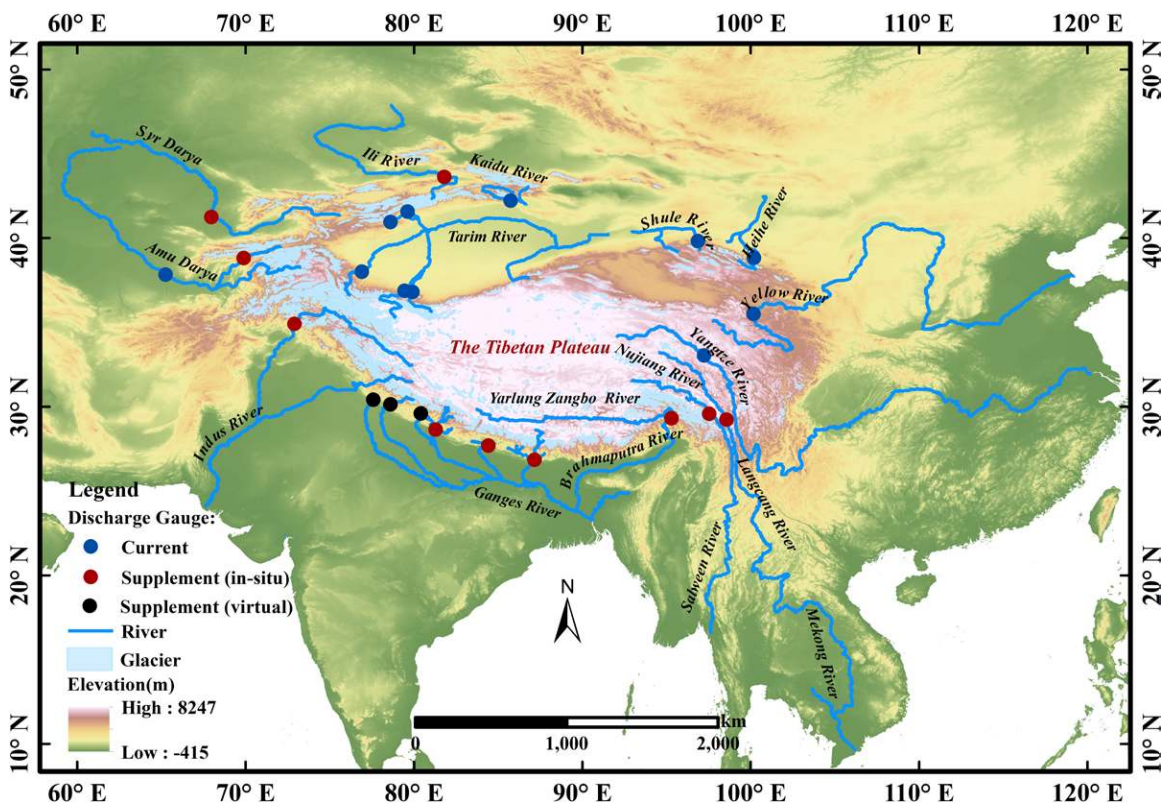

Fig. 1. Major rivers and the discharge gauges at mountain outlets (where rivers leave the mountains and enters the plains) in the Third Pole region (TP). "Current" and "Supplement" denote existing and newly built discharge gauges, respectively. The "virtual" station indicates no onsite measurement.

and Heihe Rivers) and eight transboundary rivers. The transboundary rivers are the Mekong River ("Lancang" in Chinese), the Salween River ("Nujiang" in Chinese), the Brahmaputra ("Yarlung Zangbo" in Chinese), the Ganges, the Indus River, the Amu Darya, the Syr Darya, and the Ili River. These 13 large Asian rivers straddle the westerly domain (northern and western TP region), the westerly monsoon transition domain (Yao et al. 2013b), and the Indian monsoon domain (southern TP region). Rivers in the westerly domain (Tarim, Shule, Heihe, Amu Darya, Syr Darya, Ili, and Indus) are in arid and semiarid areas in the northern and western regions of the TP, where the climate is mainly a continental climate. Meltwater from glaciers and snow constitutes the main supply of water to these rivers, which provide freshwater for many cities and regions in Central Asia. The upper basins of the Yangtze River and the Yellow River, which flow through several provinces in central China, are located in the westerly monsoon transition domain, where summer precipitation is the main driver for river runoff. The headwaters of the Brahmaputra, the Ganges, the Mekong River, and the Salween River in the southern part of the TP region, are significantly influenced by the Indian summer monsoon, and rainfall between May and October is the main driver for river runoff (Tian et al. 2007; Yao et al. 2019). In addition to differences in the spatial and temporal distribution of precipitation, driven by the influence of different large-scale circulation patterns (westerly winds and monsoon), changes in the cryosphere also regulate TRR in the TP region (Cuo et al. 2014; Bibi et al. 2018; Yao et al. 2019).

Scientific objectives. The roadmap for the TP-River project is presented in Fig. 2 and the major scientific objectives are summarized below.

1) Construct a new discharge observation network. We will construct a comprehensive discharge observation network at the mountain outlets of all eight transboundary rivers in the TP region. In situ observations from the newly built network will be valuable for the calibration and verification of cryosphere–hydrology models, and will facilitate development of improved remote sensing methods for discharge estimates, which will be useful to studies of the TP rivers.
2) Calculate reliable TRR estimates for the TP. Through combining ground-based observations of discharge with discharge estimates from remote sensing data and cryosphere–hydrology
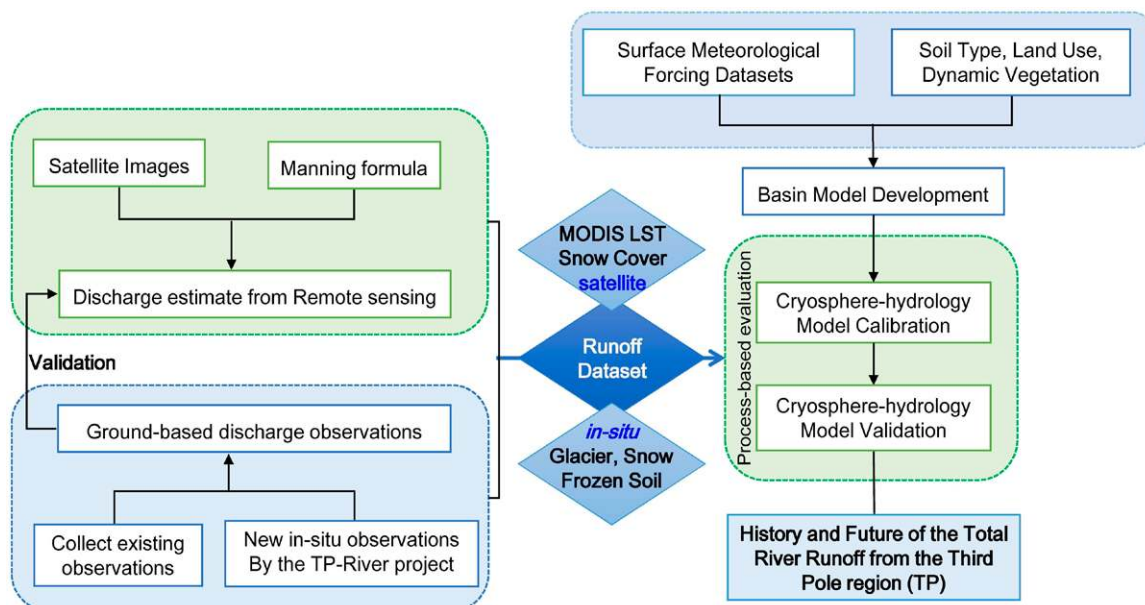

Fig. 2. Technology roadmap for the TP-River project.

modeling, we aim to accurately quantify the TRR for the 13 major TP rivers. This will make it possible to assess historical changes to the total surface water resource in the TP region, and to estimate likely future changes, providing a scientific basis for integrated water resource management for the TP and surrounding regions.

3) Identify the drivers for changes in TRR. This project will simulate and analyze changes in runoff for the major TP rivers, assessing the contribution of different drivers to the change (e.g., rain runoff, glacier melt, snowmelt, water release from soil thawing), and will assess the TRR response to changes in the westerly winds and in the monsoon.

Methods. To accurately and effectively estimate discharge for the 13 major TP rivers (five domestic rivers in China and eight transboundary rivers, each of which corresponds to different climate, topography, and glacier coverage), in situ observations, remotely sensed data, and hydrological simulations are used together to analyze annual and interannual variations in river discharge and, finally, to estimate TRR for the TP (see Fig. 2 for the roadmap). The methods used to estimate TRR for the TP in this study can be summarized as follows.

GROUND-BASED OBSERVATIONS. Regarding the eight transboundary rivers, each cross section at the mountain outlet was subdivided into segments and multiple careful measurements were made of velocity and depth, following the so-called "velocity-area method" [see Turnipseed and Sauer (2010) for details]. The Q–H rating curve was constructed from these measurements for each target cross section, where Q is river discharge and H is water level. With continuous measurements of river water levels H at these cross sections, the river discharge observations can be achieved.

DISCHARGE ESTIMATES FROM REMOTELY SENSED DATA. The environment surrounding most TP rivers and their tributaries is remote and harsh, and cross-border rivers are often under very strict local government control, making it too difficult to carry out field monitoring at some rivers and tributaries. In addition, most existing river runoff records are incomplete and include a lot missing values. Estimates of discharge from remotely sensed data are therefore a promising alternative data source and have been used to estimate river runoff at cross sections for which measurements include a considerable amount of missing data, or are completely ungauged. The TP-River project began building the TP river runoff observation network in 2018 and so using discharge estimates from remotely sensed data allows us to extend the time series to pre-2018 dates for the newly built cross sections, and to fill gaps at locations where cross sections cannot be built and maintained under the TP-River project.

The Manning formula (Manning 1889) is still used as the main principle to estimate the discharge from remotely sensed parameters:

$$Q = \frac{1}{n} R^{2/3} S^{1/2} A, \tag{1}$$

where Q is the instantaneous flow rate across a cross section (m^3 s^{-1}); A is the cross-section area (m^2); S is the hydraulic gradient of the riverbed (m m^{-1}); n is the roughness coefficient; and R is the hydraulic radius (m), which is equal to the ratio of A to the wet perimeter P_{wet}. Substituting for R, the formula can be rewritten (see also Sichangi et al. 2016)

$$Q = \frac{1}{n} S^{1/2} A^{5/3} P_{\text{wet}}^{-2/3}. \tag{2}$$

Virtual hydrology stations can be made from high-resolution remote sensing images for streams that are relatively straight and stable. At a specific virtual station (cross section), regarding wide (width ≥ 400 m) or narrow (width < 400 m) river segments, different approaches have

been proposed to estimate the daily river discharge (Wang et al. 2019). More recently, a novel method was developed based solely on remote sensing-derived parameters to estimate river discharge at small, headwater catchments in the TP with good accuracy (Kebede et al. 2020). Application of the novel method to the lower and upper reaches of Lhasa River has demonstrated reasonably good accuracies, showing the potential to quantify streamflow entirely from remote sensing imagery in these poorly gauged transboundary rivers of TP. The inputs for the novel method include mean river width that is estimated from Landsat imagery (with the modified normalized difference water index), mean depth and velocity that are calculated from empirical equations based on remote sensing, channel slope from a fine-resolution shuttle radar topography mission digital elevation model, and channel roughness coefficient through further examining Landsat images supported by literatures (Kebede et al. 2020).

In addition, regarding the large number of cloud-contaminated data at spectral imagery as well as SLC-off (scan line corrector off) images in *Landsat-7*, a new Google Earth Engine–based approach that densifies the time series of discharge by filling thin cloud-contaminated and SLC-off images, has been developed with the Landsat and *Sentinel-2* imagery. And the cloud-gap-filled and stripe-gap-filled tests are now ongoing at the Yangtze River, showing comparable performance in terms of discharge estimation with high-quality spectral images (J. Xu et al. 2021, manuscript submitted to *J. Hydrol.*).

CRYOSPHERE–HYDROLOGY MODELING. At present, it is hard to build in situ river observation stations at some ungauged international tributaries (e.g., streams in Afghanistan), and it is difficult to obtain a continuous time series of discharge from remote sensing methods due to the coarse temporal resolution of spectral and altimetry satellite images. For steep mountainous upper river basins (e.g., the Amu Darya), discharge observations from ground gauges and remote sensing can be supplemented by hydrological modeling. Modeling can simulate runoff reasonably well even for very small tributaries, and can predict future changes in river runoff if collected streamflow observations are used for careful process-based model calibration and validation.

The numerical simulation tools used in this study are physically based, distributed cryosphere–hydrology models, such as WEB-DHM (Water and Energy Budget-based Distributed Hydrological Model; Wang et al. 2009a,b,c, 2016, 2017; Shrestha et al. 2010, 2015; Zhou et al. 2015; Makokha et al. 2016; Qi et al. 2015, 2016, 2018; Qi et al. 2019; Zhong et al. 2020) and VIC-Glacier-EB (Variable Infiltration Capacity hydrology model coupled with an energy balance glacier melt scheme; Liang et al. 1994, 1996; Cherkauer and Lettenmaier 1999, 2003; Ren et al. 2018).

The VIC model (Liang et al. 1994, 1996) is a physically based, distributed hydrological model that can simulate the exchange of water and energy among soil, vegetation, and atmosphere over a grid mesh. The VIC has the capacity to simulate the hydrological processes in cold regions because it adopts a two-layer energy balance snow model and a frozen soil/permafrost algorithm (Cherkauer and Lettenmaier 1999, 2003). The VIC linked with a simple degree-day glacier melt algorithm (VIC-Glacier) has been previously used for the quantification of flow regime and composition and of runoff response to future climate changes in the TP (e.g., Zhang et al. 2013; Su et al. 2016; Kan et al. 2018; Meng et al. 2019). More recently, an energy-balance glacier scheme was coupled with the VIC model (termed as VIC-Glacier-EB; Ren et al. 2018). The coupled model was applied to a glacierized basin in the eastern Pamir, and was extensively validated with field measurements of albedo, energy fluxes, glacier mass balances, and discharge in the basin. The VIC-glacier-EB model provides a potential tool for quantifying the response of glacier melt and discharge to climate change.

The WEB-DHM (Wang et al. 2009a) is a distributed biosphere hydrological model that can consistently simulate the water, energy, and CO_2 fluxes in the soil–vegetation–atmosphere-transfer

system at the basin scale, in a distributed manner. In the past decade, the cryosphere–hydrology physics in the WEB-DHM has been continuously improved with the enthalpy-based glacier, snow, and frozen soil processes (Shrestha et al. 2010, 2015; Wang et al. 2017). More recently, for improved permafrost–hydrology simulation, the WEB-DHM has been further enhanced through parameterizing the heat and moisture exchanges between the unconfined aquifer and its upper soil layers (Song et al. 2020). The latest version of WEB-DHM cannot only simulate cryosphere melting at the point scale (e.g., Wang et al. 2017; Song et al. 2020) but also depict hydrological processes at the basin scale (e.g., Qi et al. 2019; Zhong et al. 2020).

We collect the data necessary to drive the model, including forcing data such as ground-based hydrological and meteorological observations, high-resolution reanalysis products for surface meteorology, dynamic changes in leaf area index (LAI), and fraction of photosynthetically active radiation (FPAR) for land vegetation from remote sensing products. We also use spatial input data from satellite images and field surveys, including a digital elevation model (DEM) and maps of land use and cover, soil type and properties, and glacier distribution. Additional remote sensing products are used for process-based hydrological model evaluation, for example, the land surface temperature and snow cover extent from Moderate Resolution Imaging Spectroradiometer (MODIS), as well as integrated snow depth and soil moisture products that combine point-scale ground measurements and microwave-based global monitoring.

These well-validated cryosphere–hydrology models for each river basin will be used to reconstruct historical discharges for ungauged/poorly gauged river segments with fine temporal resolution, and also to project future trends in mountain-outlet runoff for all major rivers in the TP region.

Connections to other international programs and projects. The objectives of the TP-River project, which aims to build an integrated monitoring network for runoff at the TP, are promising in part because of the project's close connection to existing international collaboration platforms.

The TP-River project (under the Pan-TPE mega-project funded by CAS) has been established following the 10-year development of the Third Pole Environment (TPE) program (Yao et al. 2012b; Yao 2014), which was initiated in 2009 by Professors Tandong Yao, Lonnie G. Thompson, and Volker Mosbrugger. Over the decade in which the TPE program has run, it has fostered and motivated a number of studies that contribute to uncovering the interactions between the atmosphere, cryosphere, hydrosphere, biosphere, and lithosphere in the TPE and surrounding regions (the so-called Pan-TPE regions).

The TP-River project also contributes to the Alliance of International Science Organizations (ANSO) initiated by CAS in 2018, which aims to promote shared development between ANSO members, including national academies of sciences, universities, research institutes, and international organizations along the "Silk Road," leading toward the achievement of the UN Sustainable Development Goals (SDGs).

Under the initiatives of the TPE program and ANSO, we have established long-term partnerships with various research institutes in the countries surrounding the TP and along the Silk Road, including Nepal, Pakistan, Kyrgyzstan, Tajikistan, Thailand, and Bangladesh. For example, since the launch of the TPE international cooperation program in 2009, the Institute of Tibetan Plateau Research, part of the CAS, has carried out many joint scientific expeditions and collaborative studies with collaborators from Pakistan, which has led to the establishment of glacial hydrology observation stations in the upper reaches of the Indus River.

Implementation of the project
Ground-based observations. Since 2017, we began to define and select hydrological cross sections at the mountain outlets for the 13 major TP rivers, which comprise eight transboundary

rivers and five Chinese rivers. For each river basin, we managed to define a region where cryospheric contributions to runoff are significant. The upper area covered by these mountain outlets is 1.66 million km², with a mean elevation of 3,660 m (see Table 1).

For the five Chinese rivers (Yellow, Yangtze, Tarim, Shule, and Heihe), discharge is routinely measured at the mountain outlets by the Ministry of Water Resources (MWR) in China using so-called "mountain outlet gauges." A long time series of quality-controlled observations from the mountain outlet gauges is therefore available from MWR for each of these five rivers.

For the eight transboundary rivers (Ili, Amu Darya, Syr Darya, Indus, Brahmaputra, Ganges, Mekong, Salween), we investigated the geology, topography, river characteristics, and hydraulic engineering in detail at the river basins, including looking at the stability of cross sections, riverbed composition, distributaries, erosion ditches, back flow, dead water, and the spatial characteristics of the hydraulic engineering. After careful consideration, we selected and built the hydrological cross sections at the mountain outlets for the eight transboundary rivers (Table 1). We equipped these hydrological cross sections with radar water level gauges and/or HOBO water level gauges (Table 2). During the field work at each cross section, the section geometry was jointly measured by a bathometer and a laser range finder, and the instantaneous flow velocity along the cross section was recorded at a distance interval using a digital flow velocity probe (Table 2 and Fig. 3). Where possible, rain gauges and automatic

Table 1. The studied TP rivers and discharge gauges at the mountain outlets. Note: "obs" denotes new gauge observations from the TP-River project, "MWR" refers to observations from the Ministry of Water Resources in China, "RS" is discharge estimation from remote sensing, and "HM" refers to discharge simulated using calibrated cryosphere–hydrology models.

Major river	Discharge gauges	Longitude (°E)	Latitude (°N)	Gauge/basin-mean elevation (m)	Methods for quantifying runoff
Yellow	Tangnaihai	100.15	35.50	2,706/4,126	MWR
Yangtze	Zhimenda	97.22	33.03	3,659/4,761	MWR
Heihe	Yingluoxia	100.18	38.82	1,709/3,669	MWR
Shule	Changmapu	96.85	39.82	2,088/3,986	MWR
Tarim	Kaqun (Yarkant)	76.90	37.48	1,438/4,283	MWR
	Shaliguilanke (Akesu)	78.60	40.95	1,909/3,460	MWR
	Xiehela (Akesu)	79.62	41.57	1,427/3,376	MWR
	Dashankou (Kaidu)	85.73	42.22	1,340/2,992	MWR
	Wuluwat (Hotan)	79.43	36.87	1,553/4,741	MWR
	Tongguziluoke (Hotan)	79.90	36.80	1,898/4,722	MWR
Ili	Karatumu	81.80	43.63	702/2,313	obs
Syr Darya	Shardara	67.97	41.24	248/1,772	obs + RS + HM
Amu Darya	Kerki	65.25	37.83	239/2,523	obs + RS + HM
Indus	Besham	72.86	34.90	1,571/4,458	obs
Ganges	Karnali	81.28	28.64	267/3,309	obs
	Gandaki	84.42	27.70	191/3,043	
	Koshi	87.15	26.86	234/3,768	
	Maha Kali	80.41	29.60	646/3,495	HM
	Upper Ganges	78.60	30.14	570/3,417	
	Yamuna	77.58	30.42	370/2,081	
Brahmaputra (Yarlung Zangbo)	Motuo	95.29	29.32	873/4,787	obs
Mekong (Lancang)	Markam	98.56	29.24	2,567/4,508	obs + MWR
Salween (Nujiang)	Rinca	97.53	29.58	2,618/4,746	obs + MWR

Table 2. The instruments used in the TP-River project.

Instrument name	Description	No. of instruments
YGRD-65 Radar water level meter (RLM)	YGRD-65 series is a pulse radar water level sensor made by Hydrospan. It can calculate the water level by sending short microwave pulse to the target and measuring the return time of the pulse. Range: 15–70 m; accuracy: ±3 mm; resolution: 1 mm; sampling interval: 30 min.	2 sets (at Ili and Brahmaputra)
HOBO U20-001-01 water level logger (WLL)	U20 adopts the principle of pressure measurement made by Onset, which can monitor water level (WL) and water temperature. Range: 0–9 m, from −20° to 50°C; accuracy: 0.5 cm, ±0.44°C (when the water temperature is 0°–50°C); resolution: 1 mm, 0.1°C (at 25°C); sampling interval: 30 min.	11 sets (at Ili, Amu Darya, Syr Darya, Indus, Ganges, Salween, and Mekong)
M9 acoustic Doppler durrent profiler (ADCP)	The SonTek RiverSurveyor system M9 made by YSI is an ADCP specifically designed to measure river discharge through measuring 3D water currents and depths from a moving vessel. 1) Flow velocity: Range: 0–20 m s^{-1}; accuracy: ±0.25%, ±0.002 m s^{-1}; resolution: 0.001 m s^{-1} 2) Water depth: Range: 0.2–80 m; accuracy: ±1%; resolution: 0.001 m.	1 set
Surface velocity radar (SVR)	SVR, commonly known as a "radar velocity gun," is made by Decatur electronics company. Range (velocity): 0.03–20.00 m s^{-1}; accuracy: ± 0.03 m s^{-1}; resolution: 0.01 m s; measurement range: 100 m; radio wave emission angle: 12°; radio frequency: 24 GHz (not susceptible to rain and fog).	1 set
Portable ultrasonic water depth sensor	Range: 100 m (at 20°C water calm target surface, larger range can be customized); accuracy: better than ±0.5% (based on the calm target surface in water at 20°C); detection blind area: ≤500 mm (small blind area can be customized); beam angle: 18° ± 2°; output signal: RS485, 4–20 mA (output two signals at the same time).	1 set
D510 laser range finder	D510 is a high precision laser rangefinder that is made by Leica. Range: 0.05–200 m; accuracy: ±1.0 mm; laser point diameter: 6/30/60 mm (10/50/100 m); angle sensor measurement range: 360°; accuracy of laser beam: ±0.2°; units: m, ft, in.	1 set
HOBO RG3-M rain gauge	The HOBO RG3-M is a self-contained tipping-bucket rain gauge which made by Onset. Collection diameter: 15.4 cm; rainfall: maximum rainfall rate (rainfall intensity) 127 mm h^{-1}; accuracy: ±1.0% (when rainfall intensity is less than 20 mm h^{-1}); resolution: 0.2 mm. Temperature: Range: from −20° to 70°C; accuracy ±0.47°C; resolution: 0.10°C.	6 sets

Table 2. (Continued).

Instrument name		Description	No. of instruments
Automatic weather station (AWS)		AWS is equipped with a cryogenic extension data collector, so it can operate continuously in a high-altitude and low-temperature environment, and automatically monitor, store, process, and transmit variables. Sampling interval: 30 min.	1 set
		05103 Wind speed and direction sensor made by R.M. Young. Range: 0–100 m s^{-1}, 0–360°; accuracy: ±0.3 m s^{-1}, ±3°.	1 set
		HMP155A relative humidity and temperature probe made by Vaisala. 1) Air temperature: Range: from −80° to +60°C; accuracy: ±0.17°C (if output with voltage signal), 0.12°C (if output with RS-485 signal) during (15°–25°C). Sensor type: Pt 100 RTD 1/3 class B IEC 751. 2) Relative humidity (RH): Range: 0.8%–100% RH; accuracy: ±1% (0%–90% RH), ±1.7% (90%–100% RH) during (15°–25°C). Sensor type: Vaisala HUMICAP180R.	1 set
		T200B Snow and rain sensor made by Geonor. Capacity: 600 mm; acquisition area: 200 cm^2; sensitivity: 0.05 mm; accuracy: 0.6 mm.	1 set
		NR01 net radiation sensor made by Hukseflux. Spectral range: 300–2800 nm (shortwave), 4.5–42 μm (longwave); Sensitivity: 5–20 μV W^{-1} m^{-2} (shortwave); 5–15 μV W^{-1} m^{-2} (longwave).	1 set
		SI-111-SS Infrared surface temperature sensor made by Apogee. Wavelength: 8–14 μm; accuracy: ±0.2°C (from −10° to 65°C), ±0.5°C (from −40° to 70°C); consistency: ±0.1°C (from −10° to 65°C), ±0.3°C (from −40° to 70°C).	1 set
		CS655 soil temperature (ST), water content (SW), and conductivity (SC) sensors made by Campbell. ST range, accuracy, and resolution: from −10° to 70°C, ±0.5°C, ±0.2°C; volumetric WS range: 5%–50%; volumetric WS precision: <0.05%; SC range: 0–3 dS m^{-1} (CS650);0–8 dS m^{-1} (CS655); SC accuracy: ±(5% × data + 0.05).	3 sets (at the depths of 10, 30, and 50 cm)
		CS106/PTB110 atmospheric pressure sensor made by Vaisala. Range: 500–1100 hPa; accuracy: ±0.3 hPa (20°C); ±0.6 hPa (0°–40°C); Resolution: ±0.01 hPa.	1 set
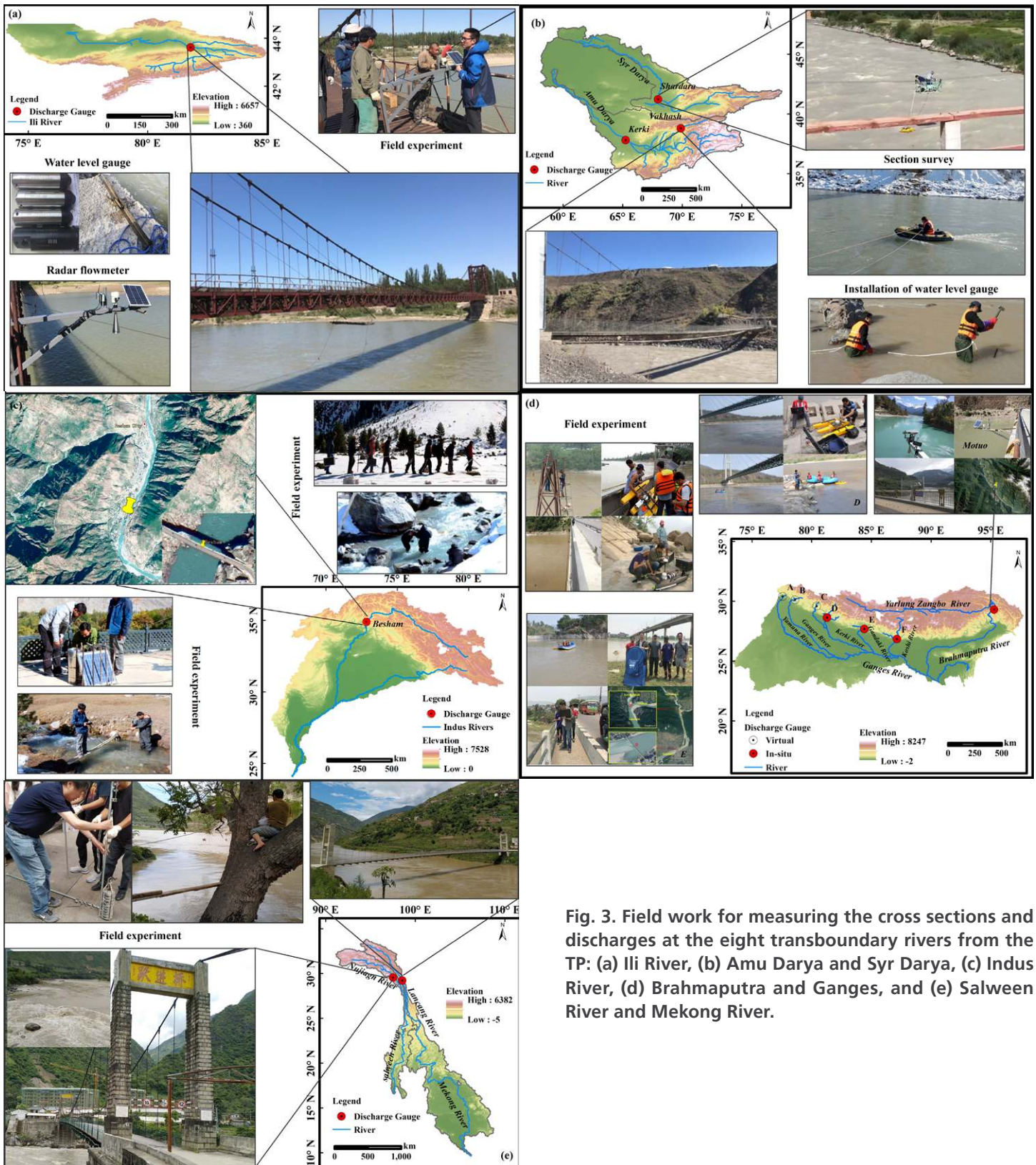
Fig. 3. Field work for measuring the cross sections and discharges at the eight transboundary rivers from the TP: (a) Ili River, (b) Amu Darya and Syr Darya, (c) Indus River, (d) Brahmaputra and Ganges, and (e) Salween River and Mekong River.

weather stations (AWS) were set up at the same elevation in the river basins where mountain outlet discharge was measured. These provide daily meteorological observations from 2018 that can be used in process-based models for hydrological simulations and projections.

Most of the field work for this study was carried out in spring 2018 and the first iteration of the river runoff monitoring network was completed in summer 2018, following the joint efforts of six research groups from two CAS research institutes over a few months (the Institute

of Geographic Sciences and Natural Resources Research and the Institute of Tibetan Plateau Research). To facilitate the installation and maintenance of field instruments for water level (discharge) measurements, the basin mountain outlet cross sections were mostly set up at nearby bridges, where radar altimetry sensors and HOBO water level sensors were installed to monitor changes in river water levels.

Remote sensing. An altimetry-based approach has been used to estimate the hydraulic parameters and river runoff for the middle reaches of the Yangtze River and discharge observations have been used to show that the method has an acceptable accuracy (Nash–Sutcliffe values > 0.5) (Sichangi et al. 2018). Although not dependent on in situ discharge observations, this method is constrained by the time resolution of available satellite altimetry images and is generally only appropriate for relatively wide rivers.

The river-width-based approach uses hydraulic–geometric methods to estimate river discharge for small- to mid-sized rivers from the effective river width extracted from spectral satellite images (e.g., from Landsat or *Sentinel-2*). This method has been used to estimate discharge for the Lhasa River and been shown to perform well (Nash–Sutcliffe values > 0.99) (Kebede et al. 2020). A precipitation-based approach, whereby an exponential filter is applied to satellite images, has been implemented for the upper Brahmaputra to estimate river runoff with fine temporal resolution. This method has been found to be accurate (Nash–Sutcliffe values > 0.92) when compared to observed discharge rates when snowmelt is considered (Zeng et al. 2020).

The satellite altimetry and river width methods for estimating discharge are complimentary and are used here to estimate daily runoff for the narrowest and widest river reaches in the TP region. The satellite precipitation-based approach, if calibrated using historical observations of discharge, can be used to reconstruct a missing time series of runoff with high temporal resolution.

Numerical simulation. We have constructed hydrological models for the upper area of the Yangtze River, the Yellow River, the Salween River, the Indus River, the Brahmaputra, the Amu Darya River, the Ili River, and for the subbasins of the Ganges using different cryosphere–hydrology models. The WEB-DHM model was run for many large rivers in the TP region, including the Yellow River (Wang et al. 2016), the Yangtze River (Qi et al. 2019), and the upper Brahmaputra (Wang et al. 2020), and the simulated runoffs are reasonable. Current ongoing work is investigating an improved version of the model, with enthalpy-based coupled snow and frozen ground physics (Wang et al. 2017), for the upper Yellow River and the upper Brahmaputra. The VIC-glacier model, designed to capture glacier-hydrology processes is currently being implemented for the upper reaches of the Amu Darya (Kerki station) and the Syr Darya (Shardara station). In the next step, these two models will be implemented to simulate and predict runoff for all major rivers in the TP region and to facilitate cross validations/intercomparisons of simulated mountain-outlet discharges.

The new observations in the TP-River project have contributed to raising the capability of hydrological simulations and to reducing the uncertainties of modeling results, which has been clearly demonstrated at the upper Brahmaputra River basin (Fig. 4). Without TP-River, all of the previous studies used the discharge observations at Nuxia gauge to perform model calibration/validation. However, this calibration cannot ensure a reliable discharge simulation at the downstream (e.g., Motuo or Pasighat), since there is a big difference in precipitation amount between upper and lower regions of Nuxia. Figure 4 shows that by using the WEB-DHM calibrated with the observed discharge at Nuxia and the integrated precipitation achieved by Wang et al. (2020), the simulated discharge still showed an obvious underestimation at Motuo with a relative error (RE) of −43%, comparing to the newly observed Motuo discharge in the

TP-River. The large discrepancy has pushed us to search for additional precipitation observations (e.g., at Motuo and Tongmai), for rechecking and correcting the precipitation at the downstream of Nuxia. With this improved precipitation, the WEB-DHM shows much improved performance at Motuo (mountain outlet of Brahmaputra), with a RE of 10% and a Nash–Sutcliffe coefficient of efficiency (Nash) of 0.65.

As a pilot modeling study, we have carefully scrutinized the multisphere interaction (atmosphere–biosphere–cryosphere–hydrosphere) and its impact on the discharge change in the upper Yangtze River basin from 1981 to 2018 (see Fig. 5 and Figs. S1–S3 in the online supplemental material), with the well-calibrated cryosphere–hydrology model WEB-DHM [see Qi et al. (2019) for model calibration/validation]. We find that significant increase in both precipitation (2.59 mm yr^{-1} or 3.56 × 10^8 m^3 yr^{-1}) and evapotranspiration (1.76 mm yr^{-1} or 2.41 × 10^8 m^3 yr^{-1}; partly caused

Fig. 4. Contributions of new observations in TP-River to raising the simulation capability and to reducing the uncertainties of results at the upper Brahmaputra River. (top) Basic watershed information, (middle) monthly precipitation at the upper area of Motuo station, and (bottom) simulated daily discharges at the Motuo station.

by the vegetation greening) has led to an insignificant increase in runoff (0.39 mm yr^{-1} or 0.54 × 10^8 m^3 yr^{-1}) in the past 38 years, showing a prominent intensification of basinwide hydrological cycle. The snow and glacier melt contributes a quarter to the total river discharge on average, but there is no prominent trend in the melting, while the frozen ground degradation exerts little influence on the runoff trend in the recent decades. It is expected that, when the TP-River project ends at 2022, our team can complete modeling work at all the 13 major rivers (partly dependent on the new observations from the TP-River) and eventually clarify the major drivers behind the changes in the TRR as integration, within the context of changing monsoon and westerly winds in the TP region.

TRR estimates for the TP. Following field work in spring and summer 2019, our team has mostly completed the instrument maintenance for the mountain outlet cross sections for the eight transboundary rivers (Brahmaputra, Ganges, Indus, Amu Darya, Salween, Syr Darya, Mekong, and Ili), and has obtained most of the annual discharge observations from 2018 (Fig. 6).
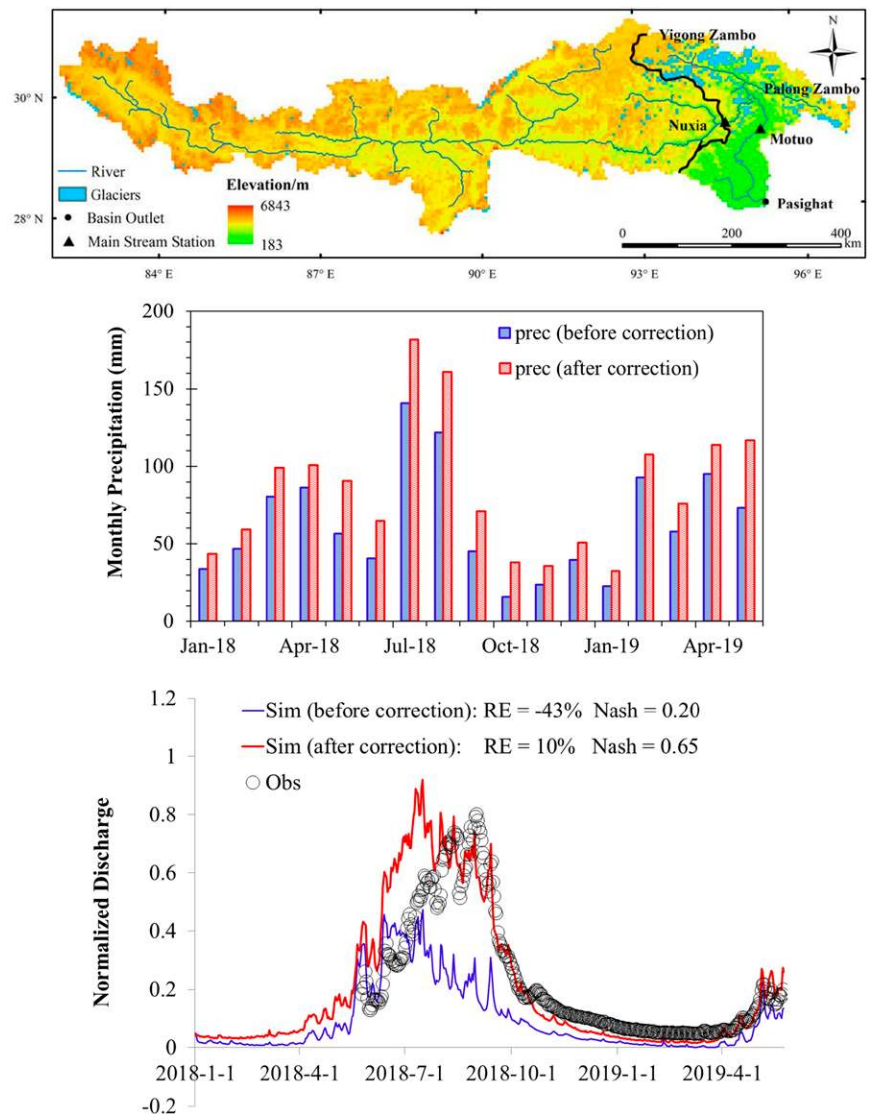
Based on these new in situ observations and discharge observations for the five Chinese rivers from the Ministry of Water Resources in China, we provide here the first estimate of annual TRR for the 13 major rivers in the TP region in 2018: 656 ± 23 billion m³. The annual river runoff at the mountain outlets varies widely between the different TP rivers, ranging from 2 to 176 billion m³, with higher values mainly corresponding to rivers in the Indian monsoon domain, rather than in the westerly domain.

The monsoon-domain rivers in the southern part of the TP region (Brahmaputra, Ganges, Salween, and Mekong) account for 61.9% of the TRR for the TP in 2018, with discharge from just two of these accounting for around half the TRR (26.9% from the Ganges, and 25.0% from the Brahmaputra). The westerly domain rivers in the northern and western parts of the TP region (Indus, Amu Darya, Syr Darya, Tarim, Ili, Heihe, and Shule) supplied an annual runoff of 201 billion m³ in 2018 (30.6% of the total TRR) to people living downstream. The greatest contributor from these rivers was the Indus River, which contributed 76 billion m³, and the lowest contribution was from the Shule River, which contributed nearly 2 billion m³. The rivers in the westerly monsoon transition domain (the Yellow River and Yangtze River), located in the eastern part of the TP region, accounted for only 7.5% of the TRR for the TP in 2018, with a combined total discharge of 49 billion m³ water.

Uncertainty in the results. We have estimated the TRR for major rivers in the TP region at the mountain-outlet locations, mostly based on ground-based gauge discharge observations. There is some
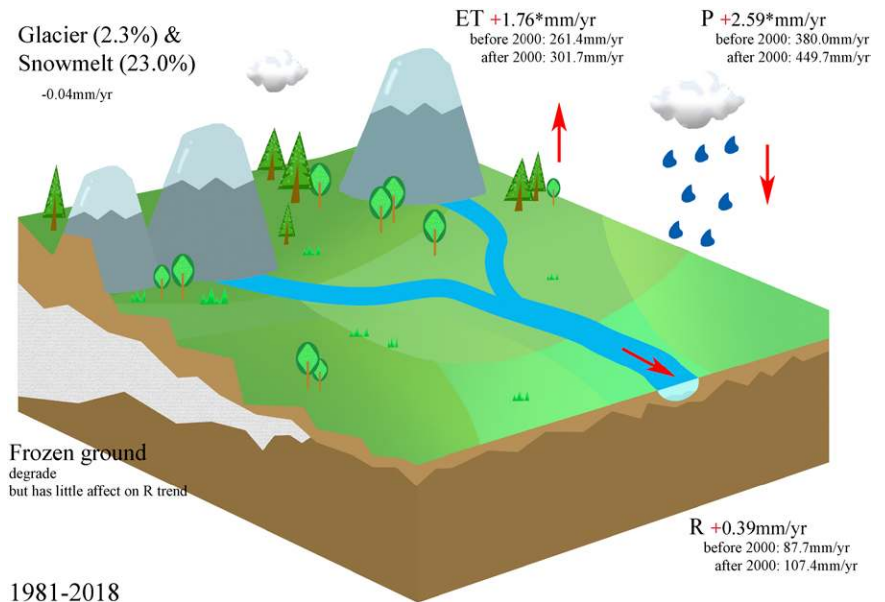

Fig. 5. A pilot cryosphere–hydrology modeling study to identify the driving forces behind the discharge change in the upper Yangtze River from 1981 to 2018. Here, significant increase in both precipitation (2.59 mm yr⁻¹; $p < 0.05$) and evapotranspiration (1.76 mm yr⁻¹; $p < 0.01$) has led to an insignificant increase in runoff (0.39 mm yr⁻¹), showing an intensified basinwide hydrological cycle. Snow and glacier melt contributes a quarter to the total river discharge on average, but there is no prominent trend in the melting, while the frozen ground degradation exerts little influence on the runoff trend in recent decades.
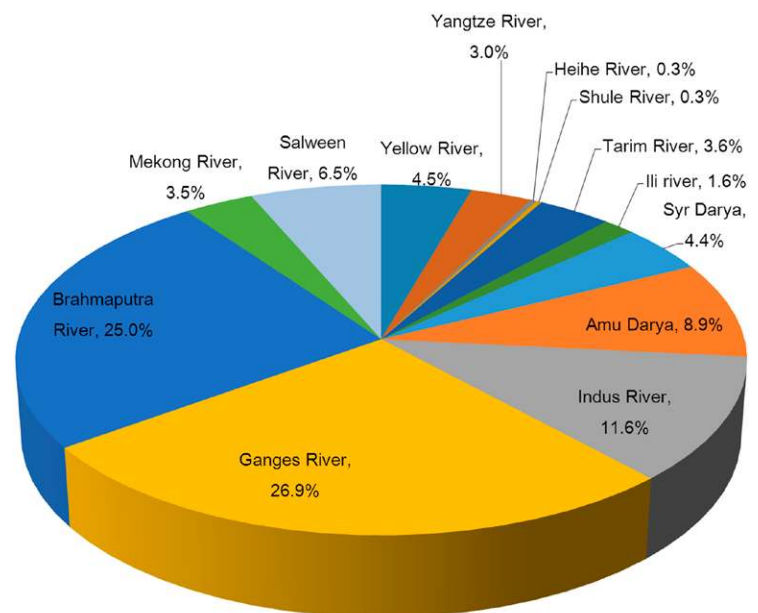
Total annual river discharges in 2018: 656±23 billion m³

Fig. 6. Annual discharge at the mountain outlets for 13 major TP rivers in 2018. The estimated total river discharge from TP is 656 ± 23 billion m³ for 2018, based mostly on ground-based observations from existing or newly built discharge gauges.

uncertainty in our TRR estimates because in situ observations from 2018 are not yet available for the Ganges (at its tributaries in India), or for the Amu Darya (at the main stream in Turkmenistan), as we cannot travel to these locations to measure runoff. We have therefore supplemented our data to account for these missing runoff data. For example, for the Amu Darya, we used an average annual value of 58 ± 15.8 billion m³, calculated from historical observations between 1953 and 1974, when anthropogenic effects are likely to have been weaker, and for three of the six tributaries of the Ganges, we used the simulated runoff by a well-calibrated cryosphere–hydrology model.

It is very difficult to carry out field observations for three tributaries of the Ganges River in India (Yamuna, Upper Ganges, and Maha Kali) because of strict local government controls, and these tributaries are likely to be subject to strong anthropogenic effects such as hydropower development and extraction for irrigation. We therefore used the simulated annual total discharge for the Yamuna, Upper Ganges, and Maha Kali, averaged over 1998 to 2007 (53 ± 7.6 billion m³; see Lutz et al. 2014), to substitute for the 2018 discharge observations. In future work, our cryosphere–hydrology model will be calibrated using the other three tributaries of the Ganges, which are in Nepal (Karnali, Gandaki, and Koshi), and the model will then be extended to the three tributaries in India to simulate discharge at virtual stations (Fig. 1). Since all six tributaries originate in the southern foothills of the Himalayas and share similar climate, topography, and basic hydrological elements, runoff simulated this way will be relatively reliable for all six tributaries.

Furthermore, emerging anthropogenic activities (e.g., water withdrawal, and reservoir and hydropower construction) at TP will influence the mountain-outlet runoff of quite a few studied rivers, with prominently large impacts on Amu Darya and Syr Darya (flowing into the Aral Sea) in the arid central Asia (see Pala 2005; Zhao and Gao 2018), while relatively small impacts on the other TP rivers (e.g., Brahmaputra, Indus, Mekong, Salween, Yellow, and Yangtze). Regarding the considerable anthropogenic impacts, this project will ultimately estimate and publicize the natural river runoff data for the Amu Darya (Kerki station) and Syr Darya (Shardara station), through process-based simulations with well-calibrated cryosphere–hydrology models. These simulations can be further compared and confirmed with the restored annual river discharges (by adding back the reported withdrawal) once they are available.

Data storage and management

Following the data policy of China and other relevant countries, we will establish and share the integrated hydrometeorological datasets for all the major TP river basins, including meteorological data (in situ observations, reanalysis, satellite-based precipitation data, etc.), remote sensing–based discharge estimates, and basinwide monthly gridded evaporation and runoff (historical and future time series; 10-km resolution for the periods 1998–2017 and 2046–65). The metadata detail the geographical locations and extents, altitudes, air temperatures, precipitation, evaporation and runoffs, which are all strictly quality controlled with the damaged and erroneous data eliminated. Relevant data are processed and stored according to the data format requirements of the National Tibetan Plateau Data Center in China (TPDC; http://data.tpdc.ac.cn/en/). So far, we have published some surface water resources products in the TPDC (e.g., upper Yellow River basin, upper Yangtze River basin, and upper Brahmaputra River basin), and users can obtain data through online registration or by contacting the author directly. Datasets from this TP-River project will be updated annually, with a 2-yr embargo period for any in situ hydrometeorological observations.

Summary

The TP-River project, as part of the Pan-TPE program of the Chinese Academy of Sciences, aims to establish a comprehensive discharge observational network at the mountain

outlets for 13 major rivers in the Third Pole (TP) region, and to quantify the total river runoff (TRR) for the TP region. In this project, ground-based observations, remote sensing methods, and numerical simulations are used in combination to quantify the TRR and to study long-term changes in TRR and the response to variations in westerly winds and monsoon.

In the first year of the TP-River project, we have almost completed construction of the infrastructure for the mountain outlet river runoff monitoring network for the TP. The observation network has been running smoothly for two years. We have collected runoff data from ungauged river reaches for two years and more data are expected to be available in the future after careful equipment maintenance and updates. The newly available in situ observations, discharge estimates from remote sensing data, and cryosphere–hydrology simulations/predictions have been used to study long-term changes to runoff and the driving forces behind these for different river basins.

However, there remains much work to do to accomplish the aims of the TP-River project.

1) We will collect and process historical mountain outlet discharge observations made prior to 2018 for all major TP rivers.
2) We will continue to explore new methods for estimating discharge from satellite data and will search for satellite imagery at finer spatial and temporal resolution to improve the accuracy of discharge estimates.
3) Based on the above, the physically based cryosphere–hydrology models will be further improved through integrating glacier, snow, and permafrost physics, so that they can be applied to the different river basins across the TP region.

In summary, this study not only provides valuable in situ observations of discharge and new technology for studying the hydrological cycle in the TP region, but also improves our understanding of water resources and water supply at the TP within the context of climate change. Multidisciplinary efforts from international research collaborations will investigate interactions between the atmosphere, biosphere, cryosphere, and hydrosphere at the TP and lead to an improved understanding of regional and global changes. This will be useful to society for mitigating against, and coping with, natural disasters and will be helpful for developing strategies for adaptation and water resource management.

References

Bibi, S., L. Wang, X. Li, J. Zhou, D. Chen, and T. Yao, 2018: Climatic and associated cryospheric, biospheric, and hydrological changes on the Tibetan Plateau: A review. *Int. J. Climatol.*, **38**, e1–e17, https://doi.org/10.1002/joc.5411.

Biemans, H., and Coauthors, 2019: Importance of snow and glacier meltwater for agriculture on the Indo-Gangetic Plain. *Nat. Sustain.*, **2**, 594–601, https://doi.org/10.1038/s41893-019-0305-3.

Chen, D., and Coauthors, 2015: Assessment of past, present and future environmental changes on the Tibetan Plateau. *Chin. Sci. Bull.*, **60**, 3025–3035.

Cherkauer, K., and D. Lettenmaier, 1999: Hydrologic effects of frozen soils in the upper Mississippi River basin. *J. Geophys. Res.*, **104**, 19 599–19 610, https://doi.org/10.1029/1999JD900337.

——, and ——, 2003: Simulation of spatial variability in snow and frozen soil. *J. Geophys. Res.*, **108**, 8858, https://doi.org/10.1029/2003JD003575.

CIESIN, 2018: Documentation for the Gridded Population of the World, version 4 (gpwv4), revision 11 data sets. NASA Socioeconomic Data and Applications Center, accessed 30 October 2020, https://doi.org/10.7927/H45Q4T5F.

Cuo, L., Y. Zhang, F. Zhu, and L. Liang, 2014: Characteristics and changes of streamflow on the Tibetan plateau: A review. *J. Hydrol. Reg. Stud.*, **2**, 49–68, https://doi.org/10.1016/j.ejrh.2014.08.004.

Immerzeel, W., L. Beek, and M. Bierkens, 2010: Climate change will affect the Asian water towers. *Science*, **328**, 1382–1385, https://doi.org/10.1126/science.1183188.

Ji, P., and X. Yuan, 2018: High-resolution land surface modeling of hydrological changes over the Sanjiangyuan region in the eastern Tibetan Plateau: 2. Impact of climate and land cover change. *J. Adv. Model. Earth Syst.*, **10**, 2829–2843, https://doi.org/10.1029/2018MS001413.

Kan, B., F. Su, B. Xu, Y. Xie, J. Li, and H. Zhang, 2018: Generation of high mountain precipitation and temperature data for a quantitative assessment of flow regime in the Upper Yarkant basin in the Karakoram. *J. Geophys. Res. Atmos.*, **123**, 8462–8486, https://doi.org/10.1029/2017JD028055.

Kang, S., Y. Xu, Q. You, W. A. Flugel, N. Pepin, and T. Yao, 2010: Review of climate and cryospheric change in the Tibetan Plateau. *Environ. Res. Lett.*, **5**, 015101, https://doi.org/10.1088/1748-9326/5/1/015101.

Kebede, M. G., L. Wang, X. Li, and Z. Hu, 2020: Remote sensing based river discharges estimation for a small river flowing over high mountain regions of the Tibetan Plateau. *Int. J. Remote Sens.*, **41**, 3322–3345, https://doi.org/10.1080/01431161.2019.1701213.

Koike, T., T. Yasunari, J. Wang, and T. Yao, 1999: GAME-Tibet IOP summary report. *Proceedings of the First International Workshop on GAME-Tibet*, A. Numaguti, L. Liu, and L. Tian, Eds., Chinese Academy of Sciences and Japan National Committee for GAME, 1–2.

Li, X., and Coauthors, 2008: Cryospheric change in China. *Global Planet. Change*, **62**, 210–218, https://doi.org/10.1016/j.gloplacha.2008.02.001.

——, and Coauthors, 2013: Heihe Watershed Allied Telemetry Experimental Research (HiWATER): Scientific objectives and experimental design. *Bull. Amer. Meteor. Soc.*, **94**, 1146–1160, https://doi.org/10.1175/BAMS-D-12-00154.1.

Liang, X., D. Lettenmaier, E. Wood, and S. Burges, 1994: A simple hydrologically based model of land surface water and energy fluxes for general circulation models. *J. Geophys. Res.*, **99**, 14 415–14 428, https://doi.org/10.1029/94JD00483.

——, ——, and ——, 1996: One-dimensional statistical dynamic representation of subgrid spatial variability of precipitation in the two-layer variable infiltration capacity model. *J. Geophys. Res.*, **101**, 21 403–21 422, https://doi.org/10.1029/96JD01448.

Luo, Y., and Coauthors, 2018: Contrasting streamflow regimes induced by melting glaciers across the Tien Shan-Pamir-North Karakoram. *Sci. Rep.*, **8**, 16470, https://doi.org/10.1038/s41598-018-34829-2.

Lutz, A., W. Immerzeel, A. Shrestha, and M. Bierkens, 2014: Consistent increase in High Asia's runoff due to increasing glacier melt and precipitation. *Nat. Climate Change*, **4**, 587–592, https://doi.org/10.1038/nclimate2237.

Ma, Y., S. Kang, L. Zhu, B. Xu, L. Tian, and T. Yao, 2008: Tibetan observation and research platform: Atmosphere–land interaction over a heterogeneous landscape. *Bull. Amer. Meteor. Soc.*, **89**, 1487–1492, https://doi.org/10.1175/1520-0477-89.10.1469.

Makokha, G., L. Wang, J. Zhou, X. Li, A. Wang, G. Wang, and D. Kuria, 2016: Quantitative drought monitoring in a typical cold river basin over Tibetan Plateau: An integration of meteorological, agricultural and hydrological droughts. *J. Hydrol.*, **543**, 782–795, https://doi.org/10.1016/j.jhydrol.2016.10.050.

Manning, R., 1889: On the flow of water in open channels and pipes. *Trans. Inst. Civil Eng. Ireland*, **20**, 161–207.

Meng, F., F. Su, Y. Li, and K. Tong, 2019: Changes in terrestrial water storage during 2003–2014 and possible causes in Tibetan Plateau. *J. Geophys. Res. Atmos.*, **124**, 2909–2931, https://doi.org/10.1029/2018JD029552.

Pala, C., 2005: To save a vanishing sea. *Science*, **307**, 1032–1034, https://doi.org/10.1126/science.307.5712.1032.

Qi, J., L. Wang, J. Zhou, L. Song, X. Li, and T. Zeng, 2019: Coupled snow and frozen ground physics improves cold region hydrological simulations: An evaluation at the upper Yangtze River basin (Tibetan Plateau). *J. Geophys. Res. Atmos.*, **124**, 12 985–13 004, https://doi.org/10.1029/2019JD031622.

Qi, W., C. Zhang, G. Fu, and H. Zhou, 2015: Global Land Data Assimilation System data assessment using a distributed biosphere hydrological model. *J. Hydrol.*, **528**, 652–667, https://doi.org/10.1016/j.jhydrol.2015.07.011.

——, ——, ——, C. Sweetapple, and H. Zhou, 2016: Evaluation of global fine-resolution precipitation products and their uncertainty quantification in ensemble discharge simulations. *Hydrol. Earth Syst. Sci.*, **20**, 903–920, https://doi.org/10.5194/hess-20-903-2016.

——, J. Liu, and D. Chen, 2018: Evaluations and improvements of GLDAS2.0 and GLDAS2.1 forcing data's applicability for basin scale hydrological simulations in the Tibetan Plateau. *J. Geophys. Res. Atmos.*, **123**, 13 128–13 148, https://doi.org/10.1029/2018JD029116.

Qiu, J., 2008: China: The third pole. *Nature*, **454**, 393–396, https://doi.org/10.1038/454393a.

Ren, Z., F. Su, B. Xu, Y. Xie, and B. Kan, 2018: A coupled glacier–hydrology model and its application in eastern Pamir. *J. Geophys. Res. Atmos.*, **123**, 13 692–13 713, https://doi.org/10.1029/2018JD028572.

Shrestha, M., L. Wang, T. Koike, Y. Xue, and Y. Hirabayashi, 2010: Improving the snow physics of WEB-DHM and its point evaluation at the SnowMIP sites. *Hydrol. Earth Syst. Sci.*, **14**, 2577–2594, https://doi.org/10.5194/hess-14-2577-2010.

——, T. Koike, Y. Hirabayashi, Y. Xue, L. Wang, G. Rasul, and B. Ahmad, 2015: Integrated simulation of snow and glacier melt in water and energy balance-based, distributed hydrological modeling framework at Hunza River Basin of Pakistan Karakoram region. *J. Geophys. Res. Atmos.*, **120**, 4889–4919, https://doi.org/10.1002/2014JD022666.

Sichangi, A. W., and Coauthors, 2016: Estimating continental river basin discharges using multiple remote sensing data sets. *Remote Sens. Environ.*, **179**, 36–53, https://doi.org/10.1016/j.rse.2016.03.019.

——, A. W., L. Wang, and Z. Hu, 2018: Estimation of river discharge solely from remote-sensing derived data: An initial study over the Yangtze River. *Remote Sens.*, **10**, 1385, https://doi.org/10.3390/rs10091385.

Song, L., L. Wang, X. Li, J. Zhou, D. Luo, H. Jin, T. Zeng, and Y. Yin, 2020: Improving permafrost physics in a distributed cryosphere-hydrology model and its evaluations at the upper Yellow River Basin. *J. Geophys. Res. Atmos.*, **125**, e2020JD032916, https://doi.org/10.1029/2020JD032916.

Su, Z., J. Wen, L. Dente, R. van der Velde, L. Wang, Y. Ma, K. Yang, and Z. Hu, 2011: The Tibetan Plateau observatory of plateau scale soil moisture and soil temperature (Tibet-Obs) for quantifying uncertainties in coarse resolution satellite and model products. *Hydrol. Earth Syst. Sci.*, **15**, 2303–2316, https://doi.org/10.5194/hess-15-2303-2011.

Su, F., L. Zhang, T. Ou, D. Chen, T. Yao, K. Tong, and Y. Qi, 2016: Hydrological response to future climate changes for the major upstream river basins in the Tibetan Plateau. *Global Planet. Change*, **136**, 82–95, https://doi.org/10.1016/j.gloplacha.2015.10.012.

Sun, A., Z. Yu, J. Zhou, K. Acharya, Q. Ju, R. Xing, D. Huang, and L. Wen, 2020: Quantified hydrological responses to permafrost degradation in the headwaters of the Yellow River (HWYR) in High Asia. *Sci. Total Environ.*, **712**, 135632, https://doi.org/10.1016/j.scitotenv.2019.135632.

Tang, Q., and Coauthors, 2019: Streamflow change on the Qinghai-Tibet Plateau and its impacts. *Chin. Sci. Bull.*, **64**, 2807–2821, https://doi.org/10.1360/TB-2019-0141.

Tian, L., T. Yao, K. MacClune, J. W. C. White, A. Schilla, B. Vaughn, R. Vachon, and K. Ichiyanagi, 2007: Stable isotopic variations in west China: A consideration of moisture sources. *J. Geophys. Res.*, **112**, D10112, https://doi.org/10.1029/2006JD007718.

Turnipseed, D. P., and V. B. Sauer, 2010: Discharge measurements at gaging stations. USGS Techniques and Methods Book 3-A8, 87 pp., https://doi.org/10.3133/tm3A8.

Wang, L., and Coauthors, 2016: Improving snow process modeling with satellite-based estimation of near-surface-air-temperature lapse rate. *J. Geophys. Res. Atmos.*, **121**, 12005–12030, https://doi.org/10.1002/2016JD025506.

——, and Coauthors, 2017: Development of a land surface model with coupled snow and frozen soil physics. *Water Resour. Res.*, **53**, 5085–5103, https://doi.org/10.1002/2017WR020451.

——, T. Koike, K. Yang, T. J. Jackson, R. Bindlish, and D. Yang, 2009a: Development of a distributed biosphere hydrological model and its evaluation with the Southern Great Plains Experiments (SGP97 and SGP99). *J. Geophys. Res.*, **114**, D08107, https://doi.org/10.1029/2008JD010800.

——, ——, ——, and P. Yeh, 2009b: Assessment of a distributed biosphere hydrological model against streamflows and MODIS land surface temperature in the upper Tone River Basin. *J. Hydrol.*, **377**, 21–34, https://doi.org/10.1016/j.jhydrol.2009.08.005.

——, ——, D. Yang, and K. Yang, 2009c: Improving the hydrology of the Simple Biosphere Model 2 and its evaluation within the framework of a distributed hydrological model. *Hydrol. Sci. J.*, **54**, 989–1006, https://doi.org/10.1623/hysj.54.6.989.

——, A. W. Sichangi, T. Zeng, X. Li, Z. Hu, and G. M. Kebede, 2019: New methods designed to estimate the daily discharges of rivers in the Tibetan Plateau. *Sci. Bull.*, **64**, 418–421, https://doi.org/10.1016/j.scib.2019.03.015.

Wang, T., D. Yang, Y. Qin, Y. Wang, Y. Chen, B. Gao, and H. Yang, 2018: Historical and future changes of frozen ground in the upper Yellow River Basin. *Global Planet. Change*, **162**, 199–211, https://doi.org/10.1016/j.gloplacha.2018.01.009.

Wang, Y., L. Wang, X. Li, J. Zhou, and Z. Hu, 2020: An integration of gauge, satellite and reanalysis precipitation datasets for the largest river basin of the Tibetan Plateau. *Earth Syst. Sci. Data*, **12**, 1789–1803, https://doi.org/10.5194/essd-12-1789-2020.

Xu, X., and Coauthors, 2008: A new integrated observational system over the Tibetan Plateau. *Bull. Amer. Meteor. Soc.*, **89**, 1492–1496, https://doi.org/10.1175/2008BAMS2557.1.

Yang, K., and Coauthors, 2013: A multiscale soil moisture and freeze–thaw monitoring network on the third Pole. *Bull. Amer. Meteor. Soc.*, **94**, 1907–1916, https://doi.org/10.1175/BAMS-D-12-00203.1.

——, H. Wu, J. Qin, C. Lin, W. Tang, and Y. Chen, 2014: Recent climate changes over the Tibetan Plateau and their impacts on energy and water cycle: A review. *Global Planet. Change*, **112**, 79–91, https://doi.org/10.1016/j.gloplacha.2013.12.001.

Yao, T., 2014: TPE international program: A program for coping with major future environmental challenges of the Third Pole region. *Prog. Geogr.*, **33**, 884–892, https://doi.org/10.11820/dlkxjz.2014.07.003.

——, and Coauthors, 2012a: Different glacier status with atmospheric circulations in Tibetan Plateau and surroundings. *Nat. Climate Change*, **2**, 663–667, https://doi.org/10.1038/nclimate1580.

——, and Coauthors, 2012b: Third Pole Environment (TPE). *Environ. Dev.*, **3**, 52–64, https://doi.org/10.1016/j.envdev.2012.04.002.

——, and Coauthors, 2013a: Cryospheric changes and their impacts on regional water cycle and ecological conditions in the Qinghai-Tibetan Plateau. *Chin. J. Nat.*, **35**, 179–186.

——, and Coauthors, 2013b: A review of climatic controls on d18O in precipitation over the Tibetan Plateau: Observations and simulations. *Rev. Geophys.*, **51**, 525–548, https://doi.org/10.1002/rog.20023.

——, and Coauthors, 2019: Recent Third Pole's rapid warming accompanies cryospheric melt and water cycle intensification and interactions between monsoon and environment: Multidisciplinary approach with observations, modeling, and analysis. *Bull. Amer. Meteor. Soc.*, **100**, 423–444, https://doi.org/10.1175/BAMS-D-17-0057.1.

Yuan, X., P. Ji, L. Wang, X.-Z. Liang, K. Yang, A. Ye, Z. Su, and J. Wen, 2018: High-resolution land surface modeling of hydrological changes over the Sanjiangyuan region in the eastern Tibetan Plateau: 1. Model development and evaluation. *J. Adv. Model. Earth Syst.*, **10**, 2806–2828, https://doi.org/10.1029/2018MS001412.

Zeng, T., L. Wang, X. Li, L. Song, X. Zhang, J. Zhou, B. Gao, and R. Liu, 2020: A new and simplified approach for estimating daily river discharge of the Tibetan Plateau using satellite precipitation: An initial study at the upper Brahmaputra River. *Remote Sens.*, **12**, 2103, https://doi.org/10.3390/rs12132103.

Zhang, L., F. Su, D. Yang, Z. Hao, and K. Tong, 2013: Discharge regime and simulation for the upstream of major rivers over Tibetan Plateau. *J. Geophys. Res. Atmos.*, **118**, 8500–8518, https://doi.org/10.1002/jgrd.50665.

Zhao, P., and Coauthors, 2018: The third atmospheric scientific experiment for understanding the Earth–atmosphere coupled system over the Tibetan Plateau and its effects. *Bull. Amer. Meteor. Soc.*, **99**, 757–776, https://doi.org/10.1175/BAMS-D-16-0050.1.

Zhao, Q., and Coauthors, 2019: Projecting climate change impacts on hydrological processes on the Tibetan Plateau with model calibration against the glacier inventory data and observed streamflow. *J. Hydrol.*, **573**, 60–81, https://doi.org/10.1016/j.jhydrol.2019.03.043.

Zhao, G., and H. Gao, 2018: Automatic correction of contaminated images for assessment of reservoir surface area dynamics. *Geophys. Res. Lett.*, **45**, 6092–6099, https://doi.org/10.1029/2018GL078343.

Zhong, X., L. Wang, J. Zhou, X. Li, J. Qi, L. Song, and Y. Wang, 2020: Precipitation dominates long-term water storage changes in Nam Co Lake (Tibetan Plateau) accompanied by intensified cryosphere melts revealed by a basin-wide hydrological modelling. *Remote Sens.*, **12**, 1926, https://doi.org/10.3390/rs12121926.

Zhou, J., L. Wang, Y. Zhang, Y. Guo, X. Li, and W. Liu, 2015: Exploring the water storage changes in the largest lake (Selin Co) over the Tibetan Plateau during 2003–2012 from a basin-wide hydrological modeling. *Water Resour. Res.*, **51**, 8060–8086, https://doi.org/10.1002/2014WR015846.